Surface and Coatings Technology, 60 (1993) 411–415

Structural analysis of sputtered $(W-C)_{1-x}M_x$ (M≡Fe,Co) films with $0 \leqslant x \leqslant 0.20$

A. Cavaleiro, B. Trindade and M. T. Vieira
Dep. Eng. Mecânica, Universidade de Coimbra, 3000 Coimbra (Portugal)

Abstract

Structural characterization of $(W-C)_{1-x}M_x$ (M≡Fe,Co) films with $0 \leqslant x \leqslant 0.20$ was carried out using electron probe microanalysis (EPMA), X-ray diffraction (XRD) and transmission electron microscopy–electron diffraction (TEM–ED). The results showed that the structure of these films depends on the percentage of iron and cobalt and becomes amorphous with increasing content of these elements. The microstructure of the crystalline coatings was found to be composed of small grains of β-WC_{1-x} with a high number of defects. A strong β-WC_{1-x} [311] texture was observed for iron and cobalt contents around 5.5 at.%. The films richer in iron and cobalt showed typical amorphous XRD and ED patterns, exhibiting two broad peaks and two wide diffuse rings respectively. Moreover, bright-field analysis revealed fairly contrasted images, the structure of these films being difficult to resolve.

1. Introduction

During the last few years there has been an increasing interest in tungsten carbide based coatings deposited by physical vapour deposition methods, as alternative materials to the traditional titanium compounds in the hard coatings market. Promising results have been achieved concerning mechanical properties, such as hardness, adhesion and wear behaviour, of W–Co–C coatings obtained by r.f. sputtering. In spite of incipient knowledge of the relationships between the mechanical and chemical properties, such as structure and chemical composition, some important conclusions concerning these aspects have already been obtained. Using X-ray diffraction (XRD) it was shown that the structure of the W–M–C (M≡Fe,Co) films depends on the percentage of iron and cobalt and it becomes progressively amorphous with increasing content of these elements [1, 2]. Moreover, the crystalline coatings were found to have higher hardness than the amorphous coatings [3]. Although no relationship was found between the type of structure and the adhesive critical load, this property, when evaluated by cohesive failure, was found to decrease with decreasing metal content [4].

Despite the increasing scientific literature concerning sputtered tungsten carbide based coatings, many questions about the structural aspects remain unanswered, in particular with respect to grain size characterization. The aim of this work was to understand in more detail the as-deposited state of the W–M–C (M≡Fe,Co) films by means of a powerful technique such as transmission electron microscopy (TEM). For this, a set of W–M–C (M≡Fe,Co) coatings with different M contents was obtained by r.f. sputtering and analysed structurally by TEM and XRD.

2. Experimental details

Thin films of W–M–C (M≡Fe,Co) were obtained by cosputtering WC–Co (0wt.% < [Co] < 15wt.%) targets and iron foils of different sizes. Films 0.1–3 μm thick were deposited onto high speed steel (M2) inserts and iron disc substrates by r.f. non-reactive sputtering, magnetron mode, with an argon pressure of 1 Pa and a bias voltage of −100 V. Prior to the depositions both substrates were sputter cleaned at −1000 V for 5 min in an argon atmosphere.

A Cameca SX50 electron probe microanalysis (EPMA) apparatus was used to determine the chemical composition of the coatings on the high speed steel substrates. The structure of the films was analysed by XRD and TEM using a Philips diffractometer, with Cu Kα radiation, and a Philips electron microscope operating at 120 kV respectively. The samples for TEM were prepared from the coatings on the iron discs. Specimen preparation consisted in a mechanical backside (iron side) thinning down to electron transparency with a Gatan dimpling device using 1 μm diamond paste, followed by ion-milling from both sides with argon ions at incident angles of 5°–11°.

3. Results

The results of chemical composition are summarized in Table 1. The percentage of impurities retained in the

0257–8972/93/$6.00

TABLE 1. Chemical composition of the coatings in atomic per cent

Target	W	C	Co	Fe	[W + M]/[C]
WC	54.3	45.7	—	—	1.19
$(WC)_{95.1}Co_{4.9}$	54.8	41.6	3.6	—	1.40
$(WC)_{90.5}Co_{9.5}$	55.5	39.4	5.1	—	1.54
$(WC)_{84.5}Co_{15.5}$	53.0	35.3	11.7	—	1.83
$(WC)_{77.6}Co_{22.4}$	46.8	35.0	18.2	—	1.86
WC + Fe	53.2	41.2	—	5.6	1.43
WC + Fe	52.0	40.7	—	7.3	1.46
WC + Fe	50.5	38.5	—	11.0	1.60
WC + Fe	49.5	34.5	—	16.0	1.89
$(WC)_{84.5}Co_{15.5}$ + Fe	43.3	35.5	14.0	7.2	1.82

films during each deposition process was not taken into account. In fact, relatively low percentages of oxygen and argon were found in all the W–M–C (M ≡ Fe,Co) as-deposited films (4 at.% oxygen and 1 at.% argon maximum values). As can be seen from Table 1, all the [W]/[C] ratios (concentrations in atomic per cent) are greater than unity, varying from 1.19 ($W_{54.3}C_{45.7}$) to 1.5 ($W_{53}C_{35.3}Co_{11.7}$). In spite of the non-existence of a direct relationship between this ratio and the chemical composition of the coatings, it increases with increasing iron and cobalt content.

Two types of diffractograms were obtained for XRD analysis (Fig. 1), depending on the composition of the coatings; one is characteristic of badly crystallized material, with relatively broad peaks indexed as β-WC_{1-x} [5], and the other is characteristic of amorphous material, with a stronger broad main peak and a weaker subpeak. The former type was obtained from films with low contents of metal addition, *i.e.* less than about 11.0 at.% M, while the latter was obtained from films with higher percentages of the element M. The presence of iron and cobalt in the crystalline coatings gives rise to preferred orientations of the β-WC_{1-x} phase (Figs. 2(a) and 2(b)). In particular, a strong [311] texture is observed for coatings $W_{55.5}C_{39.4}Co_{5.1}$ and $W_{55.3}C_{41.2}Fe_{5.6}$, *i.e.* for cobalt and iron contents close to about 5.5 at.%. The

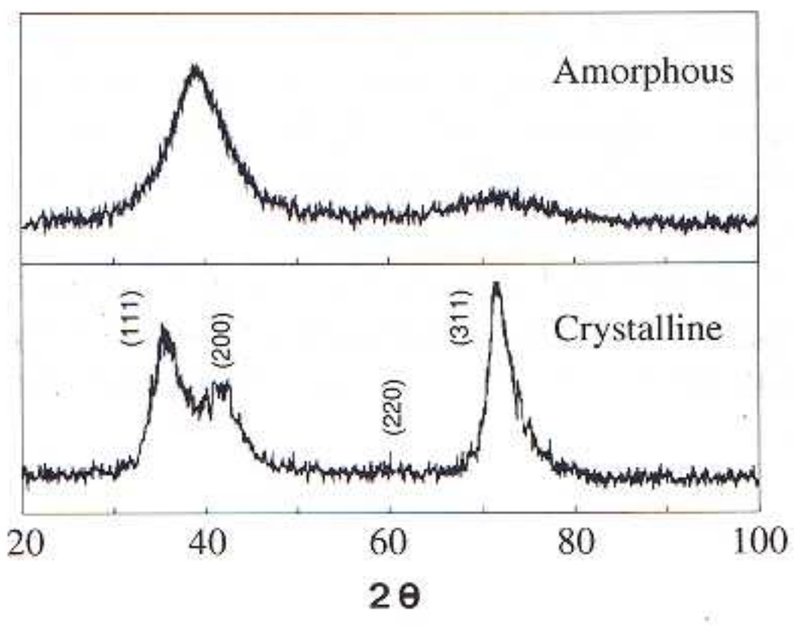

Fig. 1. Typical X-ray patterns of the crystalline and amorphous W–M–C (M ≡ Fe,Co) as-deposited coatings.

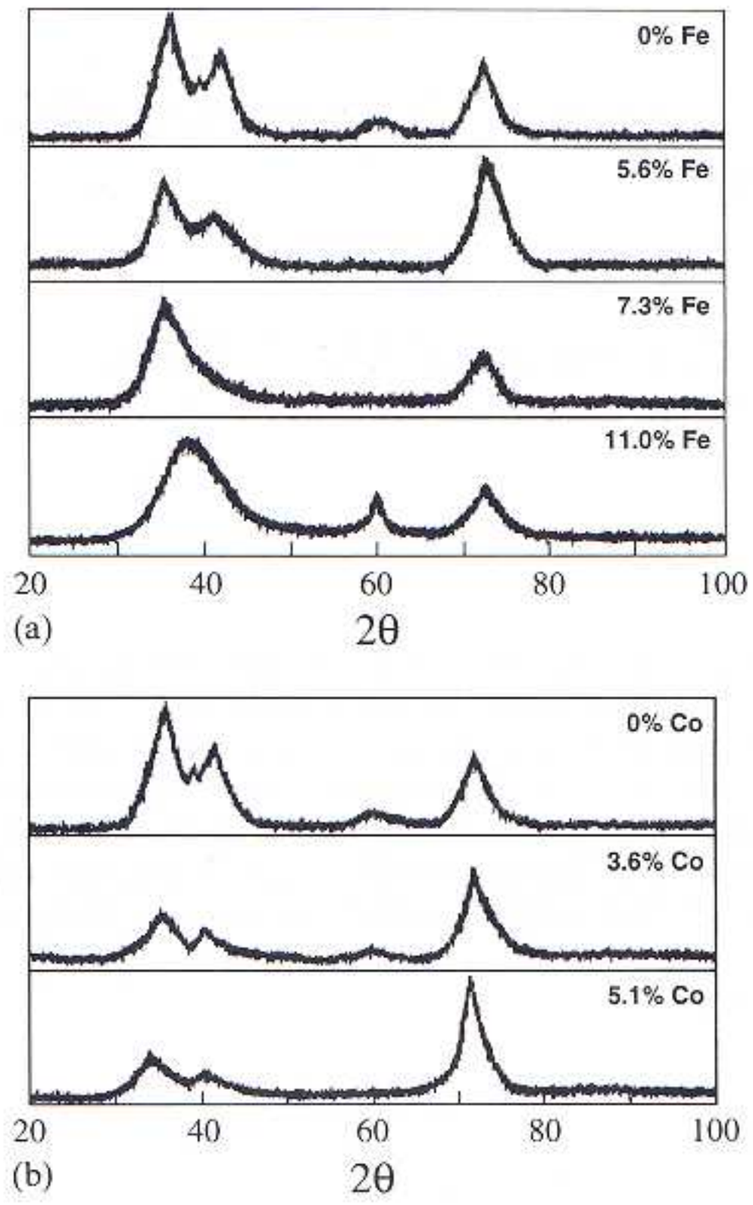

Fig. 2. Schematic XRD diffractograms of (a) W–Fe–C and (b) W–Co–C crystalline coatings.

values of the full width at half-maximum intensity of the (311) crystalline X-ray peaks correspond, according to Sherrer's equation (see for example ref. 6), to crystallite sizes of about 2–4 nm.

In agreement with the XRD results, TEM analysis showed that the structure of the W–M–C (M ≡ Fe,Co) sputtered films becomes amorphous with increasing content of iron and cobalt. Figures 3(a) and 3(b) show a bright-field image and the associated electron diffraction pattern obtained from the coating $W_{55.3}C_{41.2}Fe_{5.6}$ as a typical example of all the crystalline W–M–C (M ≡ Fe,Co) coatings. As can be seen, the microstructures of these coatings are formed by small grains of β-WC_{1-x} (some tens of nanometres in size) without any particular texture but with a high number of defects characteristic of biased films [7]. A portion of the bright ring associated with the β-WC_{1-x} (200) plane was used to form a dark-field image (Fig. 3(c)) which also reveals small "bright" spots, indicative of a fine-grain crystalline structure. Figures 4(a)–4(c) show the bright-field images of three crystalline coatings with increasing cobalt content (0 at.%, 3.5 at.% and 5.1 at.%). Comparison between these TEM images and that of the $W_{55.3}C_{41.2}Fe_{5.6}$ coating reveals similar crystallization states. For the coatings richer in the element M, the TEM bright-field analysis reveals fairly contrasted images, characteristic of amorphous material, the microstructure being very

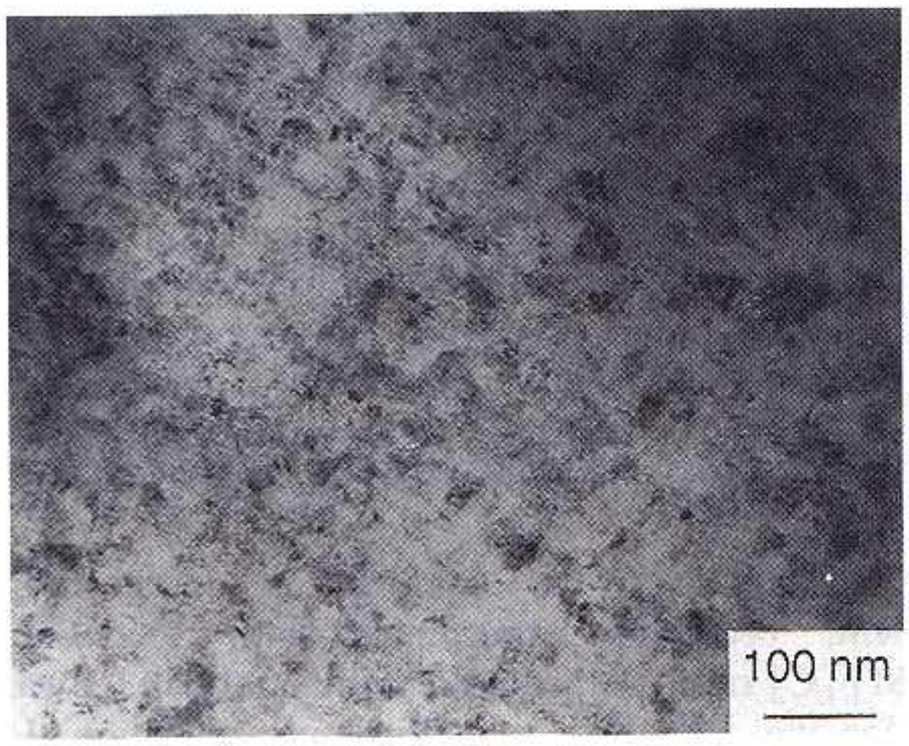

(a)

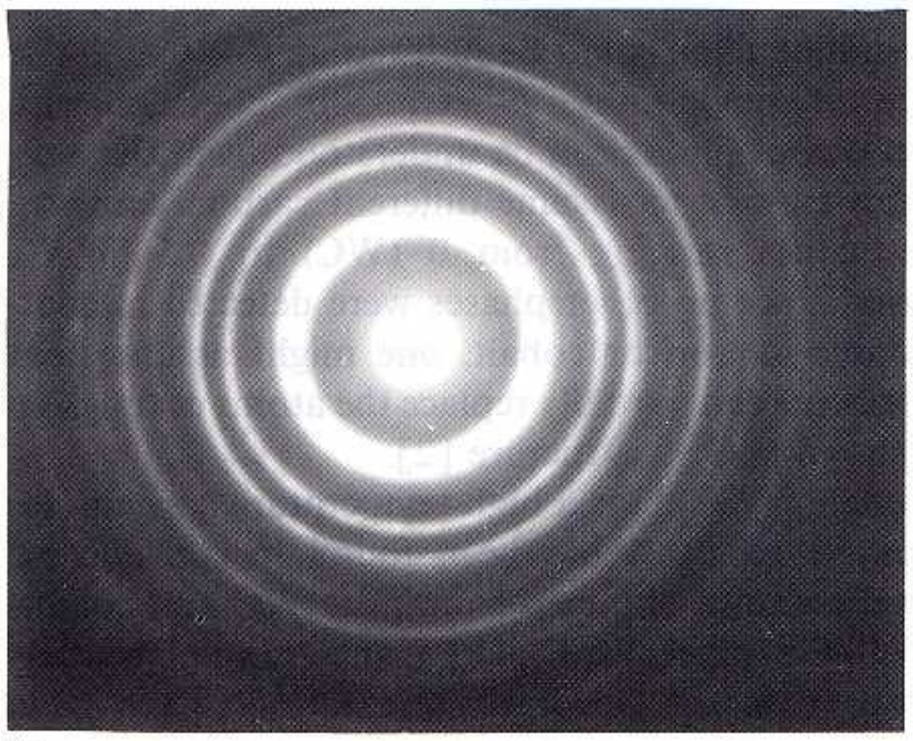

(b)

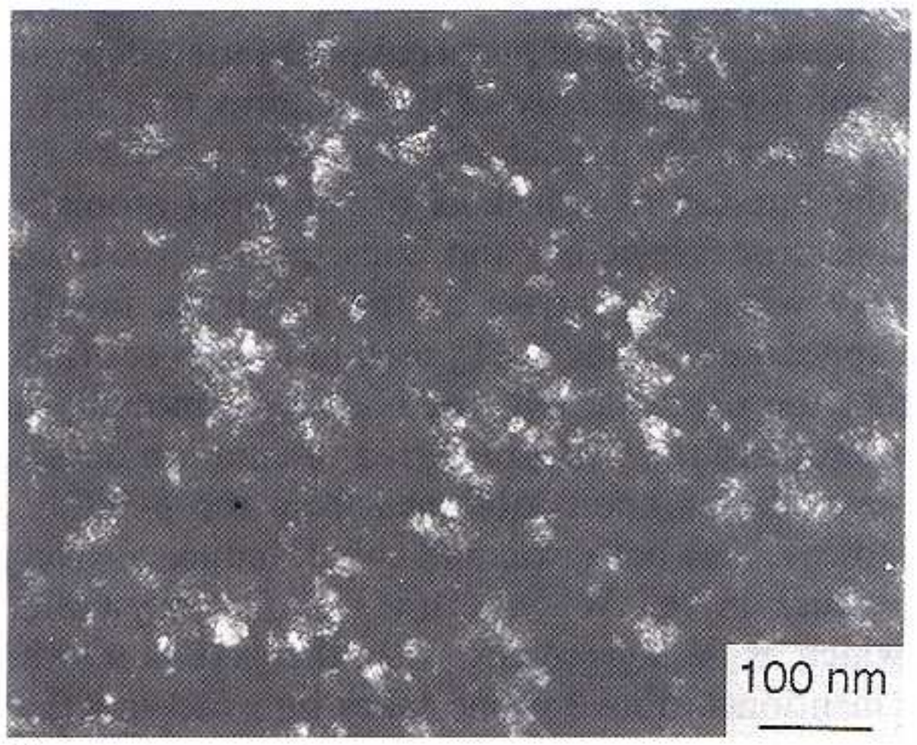

(c)

Fig. 3. Microstructure of the $W_{55.3}C_{41.2}Fe_{5.6}$ coating: (a) bright-field image; (b) electron diffraction pattern; (c) dark-field image.

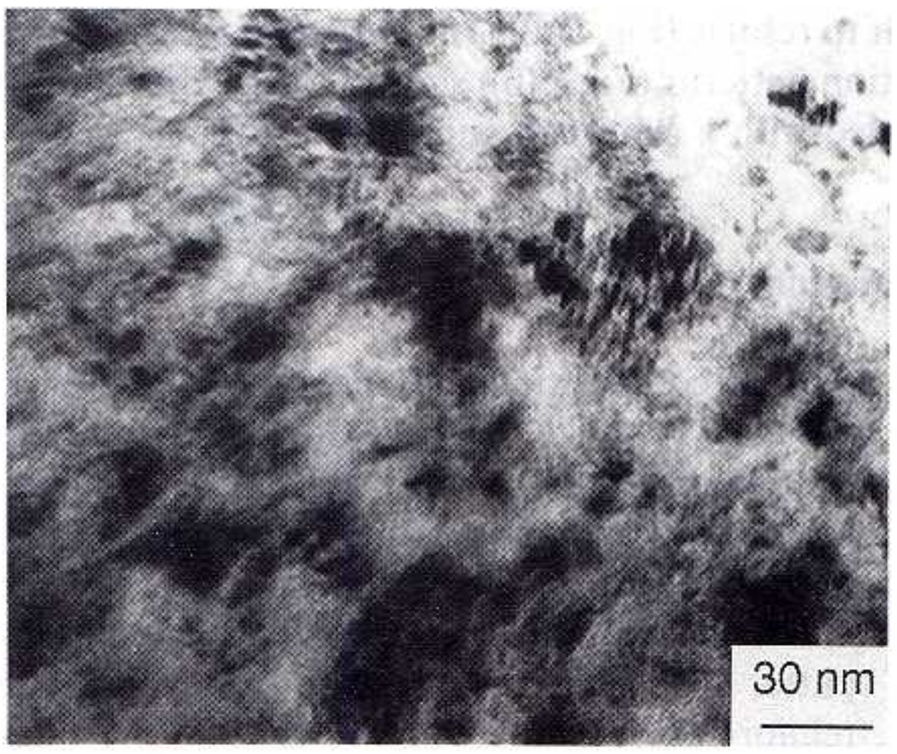

(a)

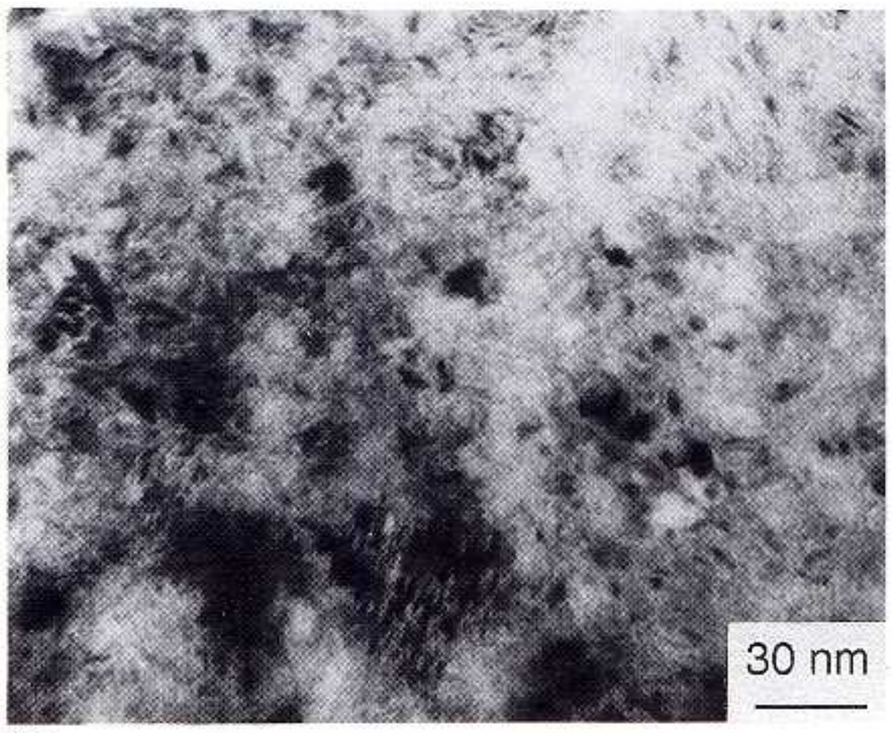

(b)

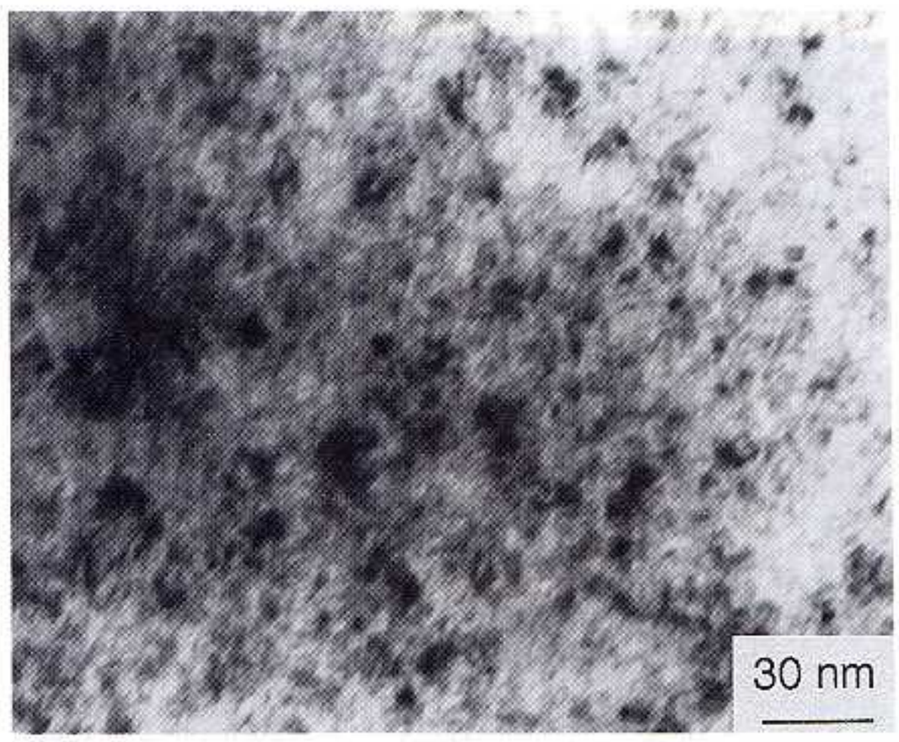

(c)

Fig. 4. Microstructure of the crystalline W–Co–C coatings: (a) $W_{54.3}C_{45.7}$; (b) $W_{54.8}C_{41.6}Co_{3.6}$; (c) $W_{55.5}C_{39.4}Co_{5.1}$.

difficult to resolve (Fig. 5(a)). The corresponding electron diffraction patterns (Fig. 5(b)) show a rather diffuse halo associated with a few weak and almost invisible rings.

4. Discussion

The chemical compositions obtained by EPMA from the as-deposited W–M–C (M ≡ Fe,Co) coatings reveal [W]/[C] ratios greater than unity and cobalt contents lower than the corresponding values in the targets as a result of the negative substrate bias. In fact, the substrate bias plays a fundamental role in the chemical composition of sputter deposited films obtained from composite targets, reinforcing the ion bombardment of the films during the deposition process. This produces preferential emission of the lighter elements (in this case carbon, iron and cobalt) and, consequently, a depletion of the films in these elements. Similar behaviour was observed in previous studies on W–C–Co films obtained from targets of tungsten carbide with different cobalt contents [1]. Concerning the impurities oxygen and argon, relatively low and constant contents were found in the as-deposited W–M–C (M ≡ Fe,Co) coatings, in accordance with what would be expected for sputtered films with substrate bias [8].

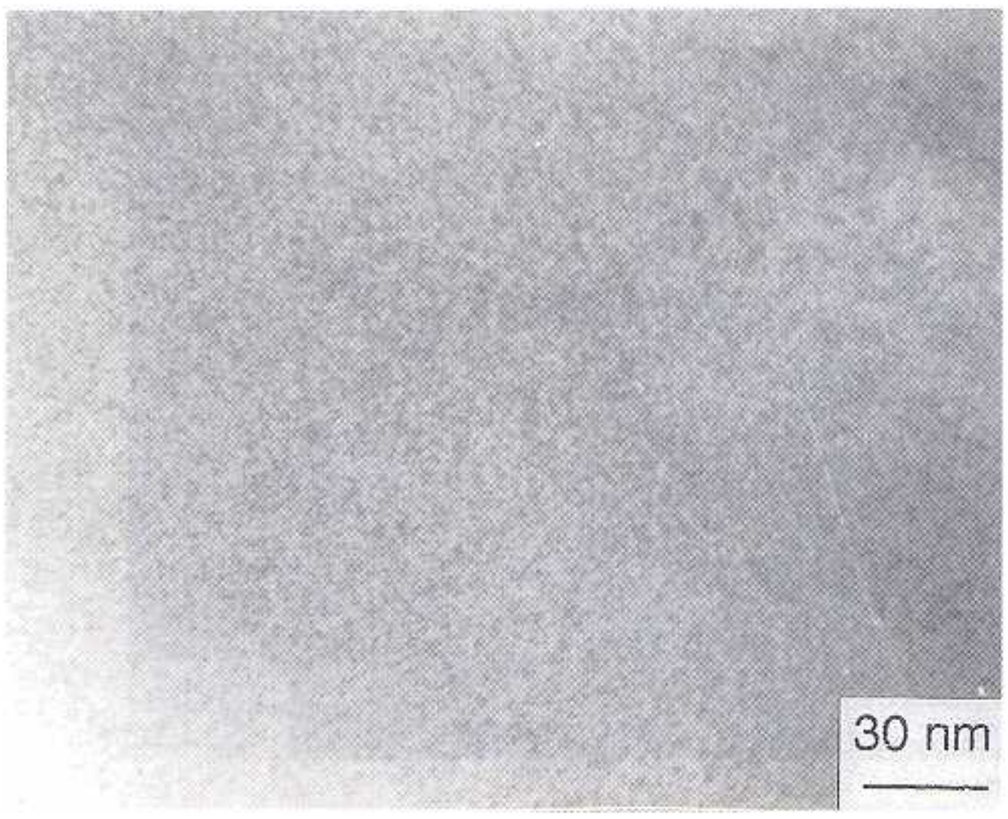

(a)

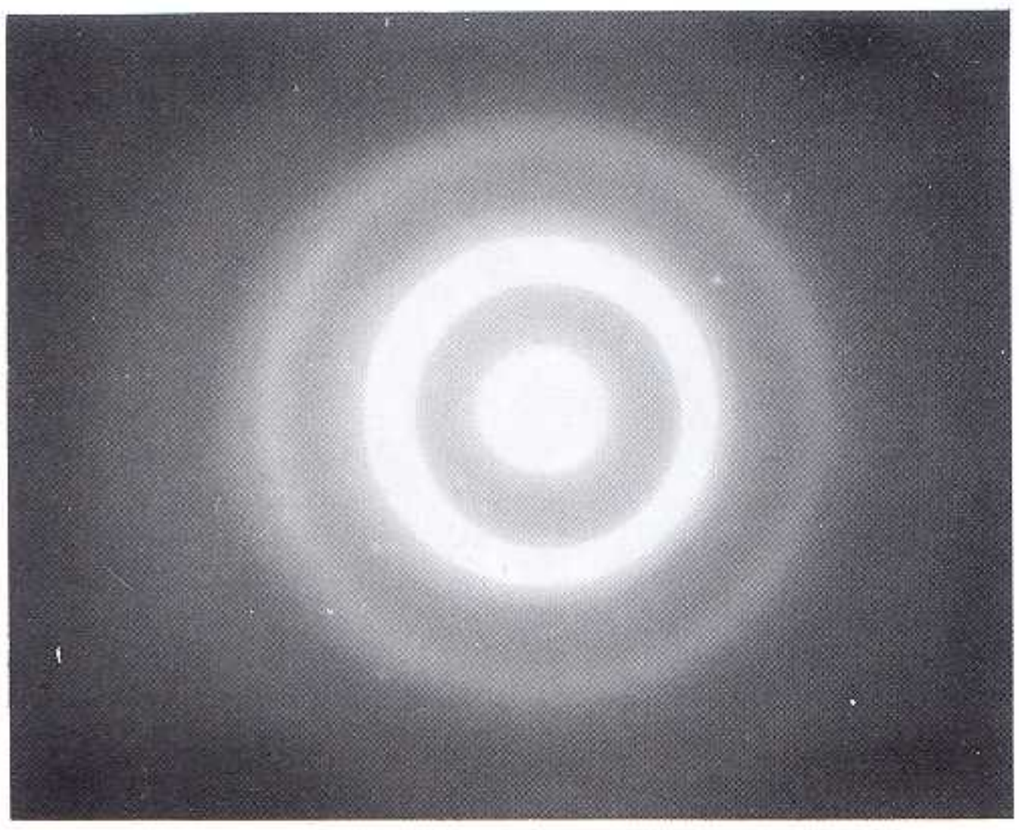

(b)

Fig. 5. Microstructure representative of amorphous W–M–C (M ≡ Fe,Co) coatings: (a) bright-field image; (b) electron diffraction pattern.

The structure of the coatings is composition dependent, becoming amorphous with increasing [W + M]/[C] ratio. A threshold value of about 1.5 was found for the crystalline to amorphous transition. In spite of the relatively broad XRD peaks and the relatively wide electron diffraction rings obtained, the structure of the crystalline films could be indexed as β-WC_{1-x}. The presence of single-phase β-WC_{1-x} in coatings with different compositions can be understood from the ability of this carbide to assume different carbon contents, with x values ranging from 0 (WC) to 0.5 (W_2C). Moreover, since no other phases were detected in coatings poorer in iron or cobalt, one might assume that these elements can partially replace the atoms of tungsten in the f.c.c. β-WC_{1-x} structure [2].

Although β-WC_{1-x} is a high temperature carbide (see for example ref. 9), it has been found in d.c. and r.f. sputtered coatings obtained from pure WC and cobalt-poor WC–Co targets [1, 10, 11]. Concerning r.f. sputtering, three different preferred orientations have been indicated for β-WC_{1-x}, changing from [111] to [311] or [100] and finally to [110] with increasing substrate bias and decreasing discharge pressure [1, 11]. According to these studies the type of preferred orientation depends on the mobility and energy of the adatoms that arrive at the substrate. The higher the discharge pressure the higher the number of collisions of sputtered atoms in the interelectrode trajectory and, consequently, the lower the energy when they arrive at the substrate, favouring the appearance of the [111] orientation. In contrast, the higher the substrate bias the higher the mobility of the adatoms, and the [110] preferred orientation occurs. The X-ray diffractograms obtained from the β-WC_{1-x} phase indicate that both iron and cobalt induce a strong [311] texture in the W–M–C (M ≡ Fe,Co) crystalline films, which is in agreement with the results of the studies mentioned above if one takes into account that a higher substrate bias corresponds to lower cobalt and iron contents in the films. The similarity between the electron diffraction and TEM bright field results obtained for both the W–Fe–C and W–Co–C coatings supports the idea advanced in a previous study [2] that these two elements play equivalent roles in the structure of as-deposited W–M–C (M ≡ Co,Fe) films.

Although there is good agreement between the TEM and X-ray results obtained for the W–M–C (M ≡ Fe,Co) coatings, slight differences concerning the grain size and texture of the β-WC_{1-x} phase were observed. In fact, some β-WC_{1-x} grains of a few tens of nanometres are visible in all the TEM bright-field images obtained from the crystalline coatings, contradicting the values from XRD analysis, in which crystallite sizes of the order of 2–4 nm were calculated from the Sherrer equation. This can be explained by the ion bombardment of the films during the deposition process. In fact, the substrate bias during film growth induces structural defects and strain effects in the W–M–C (M ≡ Fe,Co) as-deposited coatings leading to broadening of the X-ray peaks, not considered in the Sherrer formula. Because of the small grain size of the crystalline coatings it was not possible to correct these two effects by the Waren–Averbach (WA) method [12]. This method requires the use of multiple higher order reflections with reasonable intensities, which is rather difficult for films of small thickness (*i.e.* less than about 100 nm). Concerning the texture of the films, the difference between X-ray and TEM results should arise from the zone in the TEM samples under observation. In fact, owing to sample thinning, the zone transparent to electrons can refer to different points through the thickness of the film, *i.e.* to a layer close to the surface or close to the film–substrate interface, whereas in XRD the analysis integrates a substantial thickness of the film (approximately 2 μm). Studies now being carried out on the characterization of WC and $W_{55.5}C_{39.4}Fe_{5.1}$ coatings show that the preferential orientation of these films, as determined by XRD, changes with their thickness in such a way that thick films can be formed by layers with different preferential orientations. Thus, in this work, it is possible that the TEM analysis of a coating was performed in a zone preferentially oriented in a direction not coincident with the XRD texture.

5. Conclusions

The structure of the W–M–C (M ≡ Fe,Co) as-deposited coatings is composition dependent, changing from crystalline to amorphous with increasing content of iron and cobalt.

The microstructure of the crystalline coatings is characterized by small grains of β-WC_{1-x} with a high number of defects. In contrast, the coatings richer in iron and cobalt reveal microstructures characterized by a mottled appearance typical of amorphous materials.

A strong texture of the β-WC_{1-x} phase along the [311] direction is observed for iron and cobalt contents around 5.5 at.%.

TEM bright-field images obtained of crystalline films are very similar whatever the cobalt content of the films.

Acknowledgments

Sponsorship for one of the authors by Fundação Luso-Americana para o Desenvolvimento is gratefully acknowledged.

References

1 A. Cavaleiro and M. T. Vieira, *Thin Solid Films, 197* (1991) 237.
2 B. Trindade and M. T. Vieira, *Thin Solid Films, 206* (1991) 318.
3 A. Cavaleiro and M. T. Vieira, submitted to *Surf. Eng.*
4 A. Cavaleiro and M. T. Vieira, *Mater. Sci. Eng., A140* (1991) 631.
5 Joint Committee on Powder Diffraction File, *Card 20-1316*, International Center for Powder Diffraction Data, Swarthmore, PA.
6 H. P. Klug and L. E. Alexander, *X-Ray Diffraction Procedures* Wiley, New York, 1974, Chapter 9.
7 J. E. Sundgren, A. Rockett, J. E. Greene and U. Helmersson, *J. Vac. Sci. Technol. A,4* (6) (1986) 2770.
8 G. Lemperiere and J. Poitevin, *Thin Solid Films, 111* (1984) 339.
9 G. V. Raynor and V. G. Rivlin, *Phase Equilibria in Iron Ternary Alloys*, The Institute of Metals, London, 1988, p. 25.
10 E. Eser, R. E. Ogilvie and K. A. Taylor, *Thin Solid Films, 67* (1980) 265.
11 K. Fuchs, R. Rödhammer, E. Bertel, F. P. Netzer and E. Gornik, *Thin Solid Films, 151* (1987) 383.
12 B. E. Waren and B. K. Averbach, *J. Appl. Phys., 21* (1950) 595.